

低功率 YAG 激光—MAG 电弧复合焊接不锈钢

康 乐^{1,2}, 黄瑞生¹, 刘黎明¹, 刘景和²

(1. 大连理工大学 三束材料改性国家重点实验室, 辽宁 大连 116024;

2. 长春理工大学 材料科学与工程学院, 长春 130022)

摘要: 以 0Cr18Ni9Ti 不锈钢钢板为试验材料, 研究了低功率脉冲 YAG 激光—脉冲 MAG 电弧复合热源和单脉冲 MAG 焊接不锈钢。结果表明, 低功率脉冲 YAG 激光—脉冲 MAG 电弧复合热源同样具有大功率激光—电弧复合焊接才有的增加熔深、提高焊接速度、稳定焊接过程等优点; 低功率脉冲 YAG 激光的加入改变了电弧形态, 电弧根部被吸引和压缩现象显著, 提高了能量利用率; 与单脉冲 MAG 堆焊相比, 在相同焊接速度下复合焊最大能增加熔深 1.3 倍, 在相同熔深下复合焊的焊接速度可以提高 50%; 复合焊焊缝的晶粒较单 MAG 焊缝中的晶粒细小, 其焊缝抗拉强度比单 MAG 的好, 断裂属于延性断裂。

关键词: 低功率脉冲 YAG 激光; 激光—电弧复合焊接; 电弧吸引压缩; 微观组织; 延性断裂

中图分类号: TG403 文献标识码: A 文章编号: 0253—360X(2007)11—069—04

康 乐



0 序 言

自从英国伦敦帝国大学的 Steen^[1] 于 20 世纪 70 年代末提出激光与 TIG 电弧两种不同性质热源进行复合焊接技术以来, 由于激光—电弧复合焊接技术避免了单独激光焊和单独电弧焊的缺点, 具有提高焊接速度, 增强焊接接头的桥接性, 降低焊接成本等优点, 因此在随后的几十年中, 这一技术成为国际焊接界的研究热点之一^[2—9]。特别是近年来, 随着造船、汽车制造等领域的发展, 为了获得大熔深以及对厚板和铝合金等金属的焊接, 人们把注意力转移到激光—MIG/MAG 复合热源焊接这一技术上并且在实际生产中得到了应用^[6, 7]。

目前对激光—电弧复合热源焊接技术的研究主要集中在大功率激光器与电弧的复合上, 但是大功率激光器存在以下问题: 一方面其光电转换效率低(小于 3%)^[9], 激光器功率越大, 能量消耗就越大, 导致能源消耗增加; 另一方面其体积大、成本和维护费用高, 导致焊接成本提高等对实际应用不利的因素。因此各研究机构对成本低、能源消耗低的低功率激光与电弧复合热源焊接技术进行了系列的研究。在低功率激光—MIG 电弧复合热源焊接研究

方面, Shinn 等人^[8] 研究发现当激光作用点尺寸为 0.6 mm 时, 只需 200 W 的激光能量就能够实现电弧稳定燃烧。Hu 等人^[9] 采用 500 W YAG 激光与电弧复合焊接 360 钢, 研究发现熔化效率显著增加。现在激光—MIG/MAG 复合焊接集中在大功率的激光和 MIG/MAG 的复合, 应用于大厚板和铝合金等方面^[6, 7, 10], 而对低功率激光—MIG/MAG 复合焊接的研究报道很少, 因此对低功率激光—电弧复合热源焊接技术进行研究有着重要的意义。

以 0Cr18Ni9Ti 不锈钢钢板为试验材料, 对低功率脉冲 YAG 激光—脉冲 MAG 电弧复合热源焊接进行研究。对比了低功率脉冲 YAG 激光—MAG 复合热源焊接电弧和单脉冲 MAG 焊接电弧的形态, 定性分析了低功率脉冲 YAG 激光—MAG 复合热源焊接的优势, 为研究低功率脉冲 YAG 激光与脉冲 MAG 电弧的相互作用机理及推广该焊接技术应用于实际生产提供依据。

1 试 验

试验采用 LWS—500 型 YAG 固体脉冲激光器加旁轴 YD—350AG1 型 MIG/MAG 焊机进行堆焊及对接焊; 采用垂直于焊接方向的 CPL 250K CMOS 型高速摄像机对电弧形态进行实时监测, 其采样频率为 1 072 帧/s, 复合焊接示意图如图 1 所示。

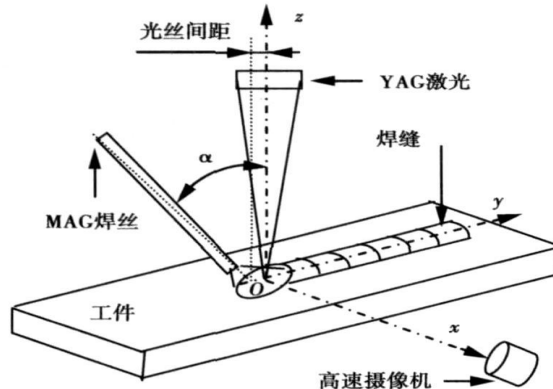


图 1 复合焊接示意图

Fig. 1 Set up of hybrid welding

试验材料为 2 mm 和 7 mm 厚的 0Cr18Ni9Ti 奥氏体不锈钢, 焊前用丙酮擦拭试件表面去除油脂, 干燥后用机械刮擦去除表面氧化膜。焊丝直径为 $\phi 1.2$ mm GB ER50—6, 焊接保护气体为 Ar(80%) + CO₂(20%), 由焊枪喷嘴喷出。将所焊试件沿垂直于焊缝方向线切割取样, 打磨、抛光、浸湿, 然后用扫描电子显微镜及附件能谱仪和光学显微镜观察和分析焊接接头的宏观形貌以及微观组织; 将对接焊的试件和母材按国家标准 GB2651—89 加工拉伸试样, 用 CCS—2205 型电子万能试验机进行拉伸测试(抗拉强度取 3 个试样的平均值), 并采用扫描电子显微镜分析断口形貌。

在试验过程中, 除了特定的变量外, 如没有特殊说明, 所用试验参数均为: 激光功率 $P = 360$ W, 保护气体的流量 $q = 20$ L/min, 激光与电弧之间的角度 $\alpha = 45^\circ$, 激光的离焦量 $\Delta z = 0$ mm。

2 试验结果及讨论

2.1 不锈钢平板堆焊试验研究

对 7 mm 厚不锈钢板材进行低功率脉冲激光复合热源和单脉冲 MAG 堆焊试验, 焊缝横截面对比如图 2 所示。从图中可以看出复合热源焊接接头熔深增加了。低功率脉冲激光复合焊的熔深是单脉冲 MAG 的 1.3 倍。

焊接速度对复合焊和单 MAG 焊熔深的影响如图 3 所示, 从图中可以看出两种焊接方法的熔深都随着焊接速度的增加而减小, 当焊接速度较小时复合焊和单脉冲 MAG 焊都比较稳定, 焊缝成形良好, 飞溅少; 当焊接速度大于 1 200 mm/min ($I = 170$ A) 时脉冲 MAG 焊接过程越来越不稳定, 甚至有时还出现断弧的现象, 而复合热源焊接过程仍比较稳定, 其

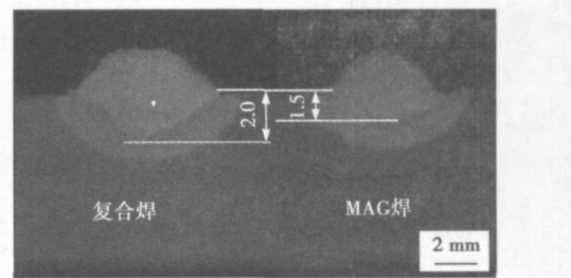


图 2 堆焊焊缝横截面对比(mm)

Fig. 2 Comparison of cross-sectional macrostructures of surfacing weld

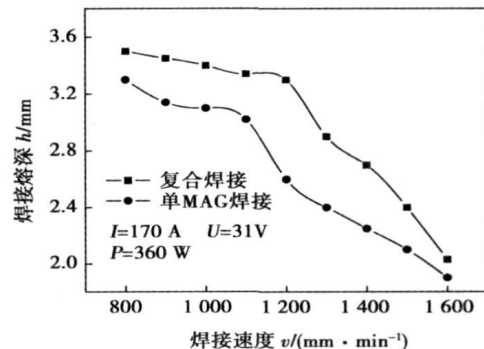


图 3 焊接速度对熔深的影响

Fig. 3 Effect of welding speed on penetration

焊接速度可以达到 1 600 mm/min ($I = 210$ A)。当复合热源焊和单 MAG 焊速相同时, 复合焊的熔深最大是单脉冲 MAG 焊的 1.3 倍。在相同的焊接条件下和试验中选定的速度范围内, 当复合热源焊和单脉冲 MAG 焊熔深相同时, 复合热源的焊接速度可以提高 50%。这表明低功率 YAG 激光—脉冲 MAG 复合热源焊接技术同样具有大功率激光—电弧复合焊接技术增加焊接熔深、提高焊接速度、稳定焊接过程等优点。

2.2 焊接电弧分析

低功率脉冲激光复合热源和单 MAG 堆焊时电弧稳定燃烧阶段的电弧形态如图 4 所示。从图 4a 与 4b, 4c 与 4d 的对比可以看出复合热源电弧根部的收缩程度比单 MAG 电弧根部的收缩程度大, 单 MAG 的电弧根部形态比较发散。这种现象的形成是因为一方面由于金属吸收激光的能量后, 熔池表面的金属强烈汽化、电离, 产生的大量光致等离子体和高温金属蒸汽电离等离子体, 提高了电弧经过激光作用点处的电导率并降低了电弧经过该路径时的电阻, 由于电弧遵守最小电压原理, 而使电弧被更稳定地吸附到激光与熔池的作用点上; 同时激光作用点处的高密度带电粒子高温区的带电粒子密度、温

度梯度进一步增大而使复合热源电弧在电弧根部被进一步强烈压缩, 电弧根部横截面的减小促进了复合热源能量的集中与增强。另一方面, 激光与熔池金属作用产生的大量光致等离子体和高温金属蒸气电离等离子体, 不仅提高了电极间的电导率, 而且与电源电场电离的等离子体一起, 在电源电场作用下定向运动; 同时, 激光作用产生的高温使电弧中心区温度升高、电弧高温区扩展及弧柱温度梯度增加, 从而增强了复合热源电弧的电子发射能力, 增大了复合热源电弧通道中的电流密度, 因此使维持电弧燃烧时的电压减小, 所以复合热源的电弧能够稳定燃烧, 电弧形态比较集中。图中 t 是电弧拍摄时间。

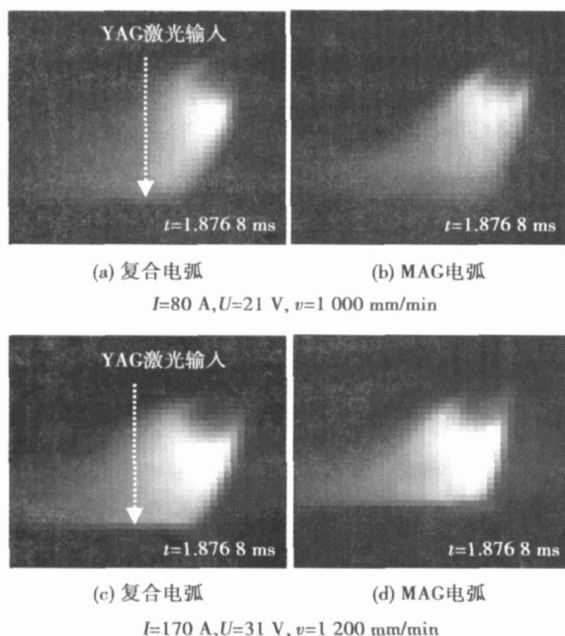


图 4 焊接电弧稳定性对比

Fig. 4 Comparison of arc stability in welding process

2.3 不锈钢对接焊试验研究

2.3.1 焊接表面成形

采用低功率脉冲激光复合热源对接焊 2 mm 的不锈钢, 实现该薄板的单面焊双面成形, 如图 5 所示。

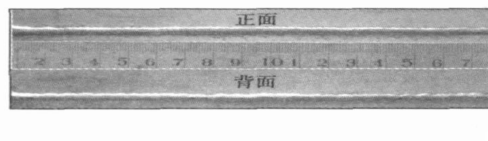


图 5 复合对接焊焊缝外观

Fig. 5 Appearance of weld for hybrid butt welding

2.3.2 焊缝组织和性能分析对比

低功率脉冲激光复合热源和单脉冲 MAG 对接焊 2 mm 不锈钢接头焊缝组织金相照片及扫描电镜照片如图 6 所示。从图 6a, c 中可以看出, 二者的焊缝组织都是由奥氏体和奥氏体晶间整齐排列的 δ 铁素体构成。但单脉冲 MAG 的焊缝中 δ 铁素体的较多, 几乎成连续的条带状分布, 晶粒也比复合焊缝中的晶粒粗大。用扫描电镜以及能谱仪分析了二者的焊缝组织及元素的成分和含量, 扫描电镜照片及能谱分析测定点的位置如图 6b, d 所示, 能谱分析结果如表 1 所示。从图 6b, d 可以看到焊缝扫描组织与金相分析的结果相一致。

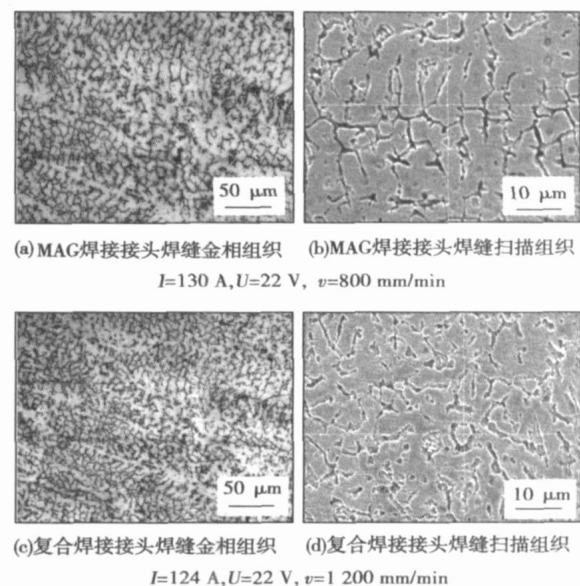


图 6 焊接接头焊缝组织

Fig. 6 Microstructures of welding

表 1 复合热源和 MAG 焊缝组织成分扫描电镜能谱分析
(质量分数, %)

Table 1 Energy spectrum analysis of weld of hybrid and MAG welding

接头	Cr	Mn	Ti	Ni	Fe
MAG 接头焊缝	19.41	0.92	0.12	9.24	70.31
复合接头焊缝	20.59	1.32	0.17	9.05	68.87

这种组织的形成是因为焊接速度提高导致焊接热输入的减少, 熔池在高温区域停留时间短, 因而焊缝金属的冷却速度大, 这有利于细小晶粒组织形成。并且从表 1 可以看出复合焊接焊缝组织晶粒中合金元素含量比单 MAG 的多。一方面由于元素含量高的合金在结晶时的成分过冷和形核率较大, 并且在晶粒长大的过程中可以阻止晶界的迁移, 防止晶粒

的长大;这也有利于细小晶粒的形成。

表 2 是 2 mm 不锈钢低功率脉冲激光复合热源和单脉冲 MAG 对接焊试样焊缝横向拉伸的结果,从表中看出复合焊接试样抗拉强度是母材的 97%;而单脉冲 MAG 焊接试样是母材的 95%。两者试样拉伸后均断在焊缝,拉伸断口 SEM 形貌如图 7 所示。从图 7a, b 看出,单脉冲 MAG 焊接试样的断口上出现小平面特征的断裂区域,而且在小平面区域之间存在撕裂棱,断裂属于准解理断裂,断口为韧脆混合断口;从图 7c, d 看出,复合试样断口上有大量韧窝并呈网状分布,断裂属于微孔聚集性型延性断裂,断口为韧性断口。这是因为复合焊接头焊缝的晶粒组织比单 MAG 焊缝的晶粒组织细小,细小的组织提高了材料的塑性、韧性等力学性能,因而在较高的焊接速度下,低功率脉冲激光复合焊接焊缝仍保持着较高的抗拉强度。

表 2 拉伸试验结果

Table 2 Result of tensile experiment

试样	抗拉强度 R_m/MPa	断裂位置
母材	631	中央
复合焊	614	焊缝
MAG 焊	601	焊缝

注:①复合热源, $I=124 \text{ A}$, $U=22 \text{ V}$, $v=1200 \text{ mm/min}$

②MAG, $I=130 \text{ A}$, $U=22 \text{ V}$, $v=800 \text{ mm/min}$

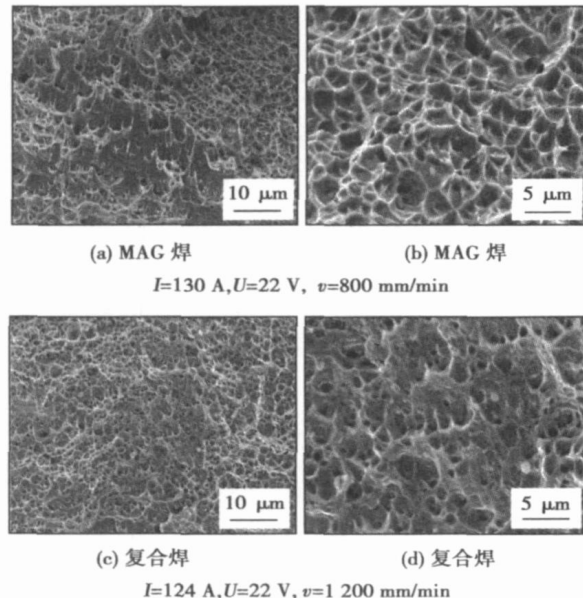


图 7 复合焊和 MAG 焊试样焊缝拉伸断口微观形貌
Fig. 7 Tensile fracture micrography of hybrid and MAG welding sample

3 结 论

(1) 低功率脉冲 YAG 激光—脉冲 MAG 电弧复合热源焊接同样具有增加熔深、提高焊接速度及提高焊接过程稳定性等大功率激光—电弧复合热源才有的特征,实际验证了低功率激光—电弧复合热源焊接技术应用于生产的可行性。

(2) 低功率脉冲 YAG 激光的加入改变了电弧的形态,电弧根部被吸引和压缩现象显著。低功率激光电弧复合焊接提高了激光和电弧之间的能量利用率。

(3) 低功率脉冲 YAG 激光—脉冲 MAG 电弧复合热源焊接焊缝的晶粒较单脉冲 MAG 焊缝中的晶粒细小,其焊缝抗拉强度比单脉冲 MAG 的好,断裂属于延性断裂。

参考文献:

- [1] Steen W M. Arc augmented laser processing of materials [J]. Appl phys, 1980, 51(11): 5636—5641.
- [2] Pace D P, Kenney K L, Galihor D L. Laser assisted arc welding of ultra high strength steels [R]. ASM Proceedings of the International Conference: Trends in Welding Research, 2002.
- [3] Dilthey U, Keller H. Prospects in laser-GMA hybrid welding of steel [R]. Proceedings of the First International WLT-Conference on Lasers in Manufacturing, Munich, 2001.
- [4] Booth G S, Howse D S, Wołoszyn A C, et al. Hybrid Nd-YAG laser/gas metal arc welding for new land pipelines [R]. Paper Presented at Pipeline Construction Technology Conference, Wollongong, NSW, Australia, 2002.
- [5] Kaierle S, Bongard K, Dahmen M, et al. Innovative hybrid welding process in an industrial application [R]. Proceedings of 19th International Congress on ICALEO 2000, Section C-ICA-LEO, 2000.
- [6] Graf T, Stauffer H. Laser-hybrid welding drives VW improvements [J]. Welding Journal, 2003, 82(1): 42—48.
- [7] Jasrau Ulf, Hoffmann Jan, Seyffarth Peter. Nd-YAG-laser-GMA-hybrid welding in shipbuilding and steel construction [J]. Robotic Welding, Intelligence and Automation, 2004, 299: 14—24.
- [8] Shinn B W, Farson D F, Denney P E. Laser stabilization of arc cathode spots in titanium welding [J]. Science and Technology of Welding and Joining, 2005, 10(4): 475—481.
- [9] Hu B, Den Ouden G. Synergetic effects of hybrid laser/arc welding [J]. Science and Technology of Welding and Joining, 2005, 10(4): 427—431.
- [10] Hyatt C V, Magee K H, Porter J F, et al. Laser-assisted gas metal arc welding of 25mm-thick HY-80 plate [J]. Welding Journal, 2001, 80(7): 163—172.

作者简介:康乐,男,1982年出生,硕士研究生。主要从事激光加工技术及其机理方面的研究工作。发表论文 2 篇。

Email: liuhn@dlut.edu.cn

the transition behavior of welding HAZ microstructure. When the cooling time $t_{8\%}$ keeps constant and $t_{12\%}$ is changed, the simulated HAZ microstructure and phase proportion vary largely. Therefore, $t_{12\%}$ is the essential factor to affect HAZ microstructure, and it is more suitable to use $t_{12\%}$ as the parameter to investigate the transition behavior of welding HAZ microstructure. The effect of the cooling time $t_{12\%}$ on the simulated HAZ microstructure is when $t_{12\%}$ increases, austenite gradually transits to branch-like morphology from band-like distribution and appears at the boundary and inside the grain. On the other hand, the ferrite content decreases with the cooling time $t_{12\%}$ increasing. In this case, austenite and ferrite in the simulated HAZ microstructure of 2205 contain more dislocation than the base metal.

Key words: duplex stainless steel; heat-affected zone; microstructure; phase proportion

Microstructure and properties of copper alloy based nano composite for spot welding electrode DENG Jingquan^{1,2}, WU Yucheng¹, Zong Yue³, WANG Wenfang¹, HUANG Xinmin¹, YU Fuwen¹(1. School of Materials and Engineering, Hefei University of Technology, Hefei 230009, China; 2. School of Materials and Engineering, Zhejiang University, Hangzhou 310007, China; 3. Materials corporation, Hefei University of Technology, Hefei 230009, China). p58—60, 64

Abstract: Copper alloy-based composites were successfully prepared using PM method with mechanically alloyed powders for spot welding electrode(CuCrZr/AlN). Microstructure and properties were characterized using transmission electron microscope, scanning electron microscope etc. Their electrical conductivity, thermal conductivity and softening temperature were measured. Results show that with the increasing of the contents of AlN, the electrical and thermal conductivity both decrease while the softening temperature increases. When the content of AlN is 0.4wt%, its softening temperature reaches 900 °C, while its electrical conductivity is about 45% IACS (international annealing copper standard) and its thermal conductivity is about 197 W/m°K. When the content of AlN is 0.2wt%, the composite has good comprehensive properties and is suitable for spot welding electrode.

Key words: Nano-composite CuCrZr/AlN; powder metallurgy; electrical conductivity; heat conductivity; softening temperature

Temperature field and stress field in arc sprayed coating of steel mold DONG Xiaoqiang, ZHANG Hongbing, LIU Yong, ZHANG Zhongli (School of Material Science and Engineering, Shenyang University of Technology, Shenyang 110023, China). p61—64

Abstract: In order to analyze the arc spraying deposition process during the mold manufacture the FEA simulation program was introduced to calculate the temperature field and stress field in the sprayed coating. The heat transfer from coating to substrate was taken into account when the mathematical model is put forward. The model is built through the micro-thickness increase of the coatings. The micro-thickness lamellas and method of element's birth or death are activated gradually to participate in the calculation. Movable

boundary condition is used to simulate the practical deposition process adequately. On the basis of the calculation, the effect of the stress distribution on the coating unstable and the residual stress is analyzed.

Key words: arc spraying; mold; numerical simulation; temperature field; stress field

Analysis for Al—Fe intermetallic compounds layer of fusion-brazed joints between aluminium and zinc coated steel by hybrid welding LEI Zhen, WANG Xuyou, WANG Weibo, LIN Shangyang (Harbin Welding Institute, Harbin 150080, China). p65—68

Abstract: The structure of Al—Fe intermetallic compounds in fusion-brazed joints between aluminium and zinc-coated steel was analyzed. Influence of welding energy input on the thickness of the Al-Fe intermetallic compounds layer was studied. And the influence of the thickness of the Al—Fe intermetallic compounds layer on the shear strength of joints was also studied. The results indicated that the intermetallic compounds layer was composed of Fe_3Al , FeAl_2 , Fe_2Al_5 and FeAl_3 , and these binary intermetallic compounds exhibited an enrichment of silicon near the weld metal side. The intermetallic compounds layer became more and more thicker along with the increasing of the welding energy input. But the effect of arc energy on the thickness of the layer was more remarkable than that of laser energy. A thinner or thicker Al—Fe intermetallic compounds layer could reduce the strength of the joints. When the the thickness of Al—Fe intermetallic compounds layer was within 1.5—4 μm , the influence of the layer on mechanical property of the joint was not significant.

Key words: laser; plused metal inert-gas arc; hybrid welding; fusion-brazing joining; Al-Fe intermetallic compounds

Low-power YAG laser-MAG arc hybrid welding of stainless steel KANG Le^{1,2}, HUANG Ruisheng¹, LIU Liming¹, LIU Jinghe²(1. State Key Laboratory of Materials Modification, Dalian University of Technology, Dalian 116024, Liaoning, China; 2. School of Materials Science and Engineering, Changchun University of Science and Technology, Changchun 130022, China). p69—72

Abstract: This paper studied the low-power pulsed YAG laser-pulsed MAG arc hybrid welding of stainless steel based on the comparison between hybrid welding process and single pulsed MAG (metal active gas) arc welding. Compared with high-power laser-arc hybrid welding, the low-power pulsed YAG laser-pulsed MAG arc hybrid welding also had many same merits such as increasing penetration depth, improving welding speed and stabilization of welding process. The shape of the arc was changed in low-power pulsed YAG laser hybrid welding due to the input of low-power pulsed YAG laser. When the pulsed YAG laser acted on arc region, the attraction and contraction of the arc root in low-power pulsed YAG laser-pulsed MAG arc hybrid welding was prominent, and the energy absorption of MAG arc and pulsed YAG laser increased. The penetration depth in low-power pulsed YAG laser-pulsed MAG arc hybrid welding was 1.3 times of that in MAG welding when welding speed was same, and the welding speed increased 50 percent when the penetration depth was equal to that of MAG welding. The crystal grain of hybrid

welding was smaller than that of weld for MAG welding, and the strength of hybrid welded joint was higher than that of MAG welded joint, and hybrid welded joint rupture was ductile nupture.

Key words: low-power pulsed YAG laser; laser-arc hybrid welding; arc attraction and contraction; microstructure; ductile nupture

Effects of Ce on spreadability of Sn—Cu—Ni lead free solder and mechanical properties of soldered joints SHI Yiping¹, XUE Songbai¹, WANG Jianxin¹, GU Liyong², GU Wenhua² (1. College of Materials Science and Technology, Nanjing University of Aeronautics and Astronautics Nanjing 210016, China; 2. Changshu Huayin Filler Metals Co. Ltd., Changshu 215513, Jiangsu, China). p73—77

Abstract: Effects of rare earth Ce on spreadability of Sn—Cu—Ni solder on copper, mechanical properties of soldered joints and the microstructure of Sn—Cu—Ni—Ce solder were investigated respectively. The results indicate that with the increase of the content of Ce added to the Sn—Cu—Ni solder, the spreading area of Sn—Cu—Ni—Ce solder on copper was enlarged. When the content of Ce is about 0.05%, the spreading area is the largest and the microstructure of Sn—Cu—Ni solder is fine and uniform, and the mechanical properties of soldered joints are improved observably. Experimental results also show when the content of Ce is over 0.05%, the grains of the solder gradually become coarse, the spreadability of the solder descend, and the mechanical properties of soldered joints deteriorate as well.

Key words: Sn—Cu—Ni—Ce solder; lead-free solder; spreadability; mechanical properties; microstructure

Influence of ultrasonic peening treatment to gray cast iron welding cold crack YAN keng NIE jie, YU huaidong, XU Lv (Provincial key Lab of Advanced Welding Technology, Jiangsu University of Science and Technology, Zhenjiang 212003, Jiangsu, China). p78—80, 84

Abstract: To study the influence of ultrasonic peening treatment to welding cold crack, the tests were conducted on the specimens made of gray cast iron. Research focused on restraint stress and quenched structure of the three main reasons to induce the welding cold crack. Test method of cold crack was slit type cracking test. The test results show that by peening the whole weld on the one hand, the ultrasonic peening treatment can reduce the residual stress at the most degree. That is the residual stress R_1 are—53 and—57 MPa, R_2 are—37 and—80 MPa on the two specimens weld. On the other hand, the ultrasonic peening treatment can accelerate to form the nodular graphite cast iron and eliminate white cast iron, and the weld is made of nodular graphite cast iron after ultrasonic peening treatment. The reasonable ultrasonic peening treatment can absolutely avoid welding cold crack by reduce the residual stress and quenched structure.

Key words: ultrasonic implement treatment; residual stress; welding cold cracking

High-frequency pulse modulated variable polarity welding power and its arc pressure QIU Ling, FAN Chenglei, LIN Sanbao,

YANG Chunli (State Key Laboratory of Advanced Welding Production Technology, Harbin Institute of Technology, Harbin 150001, China). p81—84

Abstract: A novel variable polarity welding power with high-frequency pulse modulation is designed by means of superimposed circuit, which can produce arc characteristics of high-frequency pulse welding in variable polarity welding process. Based on mathematic model of arc pressure and process experiment, the high-frequency pulsed current can increase arc pressure in a large scale. In the same root-mean-square welding current, the arc pressure with high-frequency (5 kHz) pulsed current increase to 2 times of the normal tungsten inert-gas welding arc, and it helpful for increasing of arc stiffness and energy density. It also provides theoretical proof for further researches on the high-frequency pulse modulated variable polarity welding.

Key words: variable polarity welding; high-frequency pulse current welding; arc characteristics; arc pressure

Numerical simulation of creep behavior of SnAgCu-CNT lap shear solder under thermal cycles HAN Yongdian¹, JING Hongyang¹, XU Liaryong¹, WEI Jun², WANG Zhongxing³ (1. School of Materials Science and Engineering, Tianjin University, Tianjin 300072, China; 2. Singapore Institute of Manufacturing Technology, 71 Nanyang Drive 638075, Singapore; 3. Bulter (Tianjin) Inc. Tianjin 300457, China). p85—88, 92

Abstract: Distribution of creep strain and stress of SnAgCu-CNT lap shear solder was studied under conditions of 125—40 °C by means of finite element method (FEM). The results show that obvious shearing deformation is found on the lap solder after 4 thermal cycles, then is the visible displacement on the upper and lower surfaces. Maximum equivalent creep strain lies in the middle of length orientation of solder pad surfaces, while minimum strain lies in the center of solder. FEM results coincide well with experiment results. The curve of equivalent creep strain and stress versus time in the node of maximum equivalent creep strain exhibit apparent periodicity and build-up effect.

Key words: finite element method; SnAgCu-CNT; lap solder; equivalent creep strain

Igniting pattern of plasma-MIG welding Li Deyuan, Zhang Yishun, Dong Xiaoqiang (School of Materials Science and Engineering, Shenyang University of Technology, Shenyang 110023, China). p89—92

Abstract: In order to analyze the arc igniting course of the plasma-MIG(metal inert-gas) dual-arc welding, Paschen law was introduced to calculate the breakdown voltage on the different arc igniting paths. The effect of disruptive distance and temperature on the arc ignition was studied. The pattern that the plasma arc ignites by means of the breakdown path provided by the MIG arc was proved. It has been shown that the temperature and type of the shield gas must be taken into account when the lowest breakdown voltage on different igniting path was compared. Paschen law is suitable for analyzing the effect of these parameters and can be used to predict the igniting path of the second arc. The method can also be used to other